Supporting Information.

Direct Conversion of Silver Complexes to Nanoscale Hexagonal Columns on Copper Alloy for Plasmonic Applications

Yuko S. Yamamoto*, Katsuyuki Hasegawa, Yuki Hasegawa, Naoshi Takahashi, Satoshi Fukuoka, Norio Murase, Yoshinobu Baba, Yukihiro Ozaki, and Tamitake Itoh*

*E-mail: ys-yamamoto@aist.go.jp and tamitake-itou@aist.go.jp.

(1) XPS spectrum of sulfer and oxygen in NHCs

Figure S1 shows typical XPS spectra of inside NHCs. The spectra certainly show peaks of S 2p and O 1s, indirectly showing thiosulfates on NHCs. However, these peaks are too small to assign the chemical states of S and O atoms on NHCs.
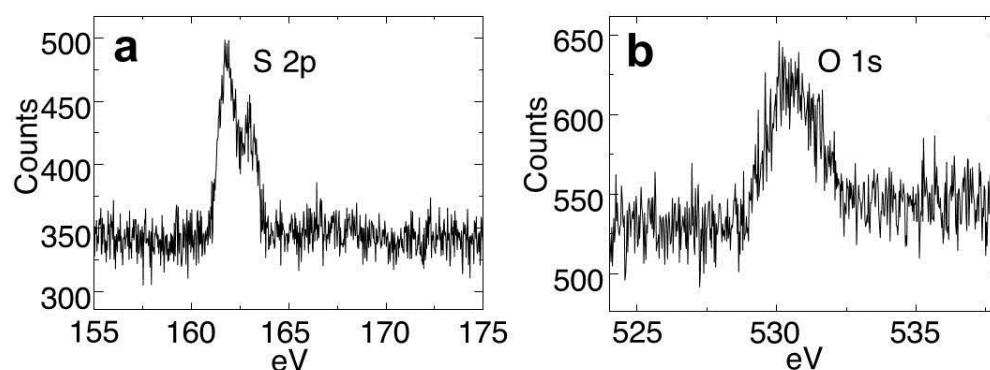

Figure S1. Typical XPS spectra of (a) sulfur and (b) oxygen inside NHCs. These high resolution spectra (50 scans, 40 sec/spectrum) were recorded with a 24-eV pass energy,

(2) SERS spectra of NHCs

Figures S2a and S2b show a SERS mapping image and the averaged Raman spectrum of the NHCs, respectively. These bands are suppressed when the aqueous dye solution (R6G or CR) is added to the NHCs, as shown in Figures 2f and 2g in the manuscript. Figure S2c compares the Raman spectrum of sodium thiosulfate and the SERS spectrum of NHCs. The differences between these spectra confirm that the Raman bands of the NHCs are not associated with those of sodium thiosulfate, suggesting that thiosulfate ions form complex with NHCs.

Table 1. Characteristic Raman vibrational modes and assignments of sodium thiosulfate.

Sample	Peak shifts (cm^{-1})	Assignment
Sodium thiosulfate (solid) [1,2]	323 (m)	S-S-O op bend
	432 (s)	S-S sym str
	542 (w)	O-S-O asym bend
	628 (sh)	O-S-O sym bend
	670 (m)	O-S-O sym bend
	1015 (m)	S-O sym str
	1118 (w)	S-O asym str
	1164 (w)	S-O asym str

s = strong; m = medium; w = weak; sh = shoulder; op = out of plane; str = stretching; sym = symmetric; asym = asymmetric.
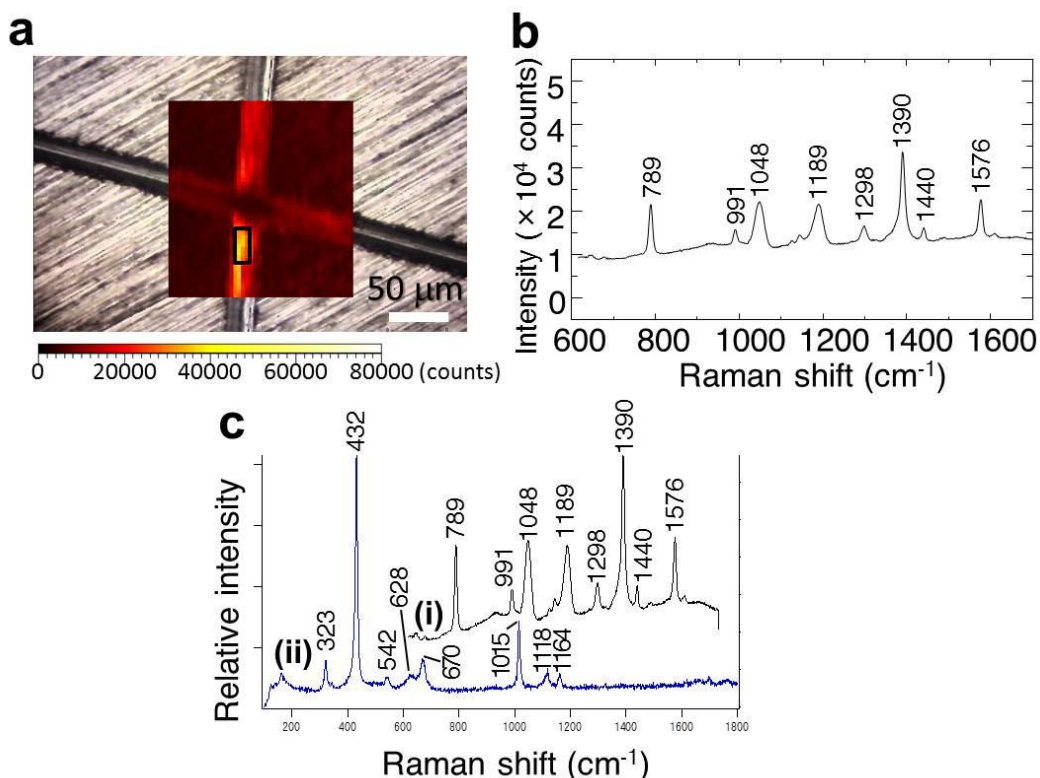
1

Figure S2. (a) SERS mapping images of NHCs at 1390 cm^{-1}. (b) Averaged SERS spectrum of NHCs. For the averaged spectrum, spectra from inside the black square within the scratch in Figure S1a were averaged. (c) Comparison of (i) SERS spectrum of NHCs and (ii) Raman spectrum of sodium thiosulfate (solid). These spectra are offset for clarity.

(3) Estimation of SERS enhancement factors of R6G and CR on NHCs

SERS enhancement factors (EFs) can be estimated by dividing the SERS intensity of the substrate with NHCs by conventional Raman intensity obtained without NHCs, according to the calculation for the analytical EF (AEF).[3] Thus, we measured the SERS and the conventional Raman spectra of each dye on the substrates as shown in Figures 2f and 2g, respectively. Unfortunately, the intensity of the conventional Raman spectra of the dyes is too weak to be identified (Figure 2f (ii), 2g (ii)). The weak conventional Raman spectra indicate that SERS signals are exclusively from dye molecules adsorbed on NHCs. However, the lack of Raman signals prevents us from estimating absolute values of EFs. Thus, using the minimum amount of detectable signal counts (~30) as Raman signals we tentatively estimated quasi-EFs of R6G and CR. They are 10^3 and 10^2, respectively. The estimated quasi-EFs are from within mapping areas of the substrates (~100 μm^2) and are not those of single SERS hot spots (~several nm^2). Thus, the EF values of $>10^3$ for R6G are reasonable compared with those previously reported.[4-6]

The present EFs cannot be directly compared with the reported ones of up to 10^{10} obtained from isolated silver nanoparticle dimers.[7] It is a common issue in the development of practical SERS substrates. The EM enhancement is a product of spatial and temporal increases in EM interactions between photons and molecules due to plasmon resonance,[8] as is explicitly described in the EM enhancement mechanism.[7,9] The spatial increase corresponds to plasmonic focusing of the photons on a local area of the substrate. Thus, in the SERS measurement, the contribution of the spatial increase to the EF is suppressed when EFs are averaged over a large area. The temporal increase corresponds to a prolonged stay of the photons on the substrate. The temporal increase is quantified using a Q factor, which is

2

intrinsically low, ~10, because of ultrafast dephasing of the plasmon polariton.[10] Thus, we consider that the present EF values are comparable to those of standard SERS substrates.

(4) Evaluation of number of hot spots on NHCs

The crevices within the focal spot (1.93 µm^2) were counted for each reaction time using the SEM images in Figures 3a–3d, as shown in Figure S3. The crevices are marked with red lines in each panel. We selectively counted the crevices formed where the NHCs contact each other and excluded the NHCs separated from each other, because EM fields at the hot spots are localized within ~1 nm, which is below the spatial resolution of the SEM images.
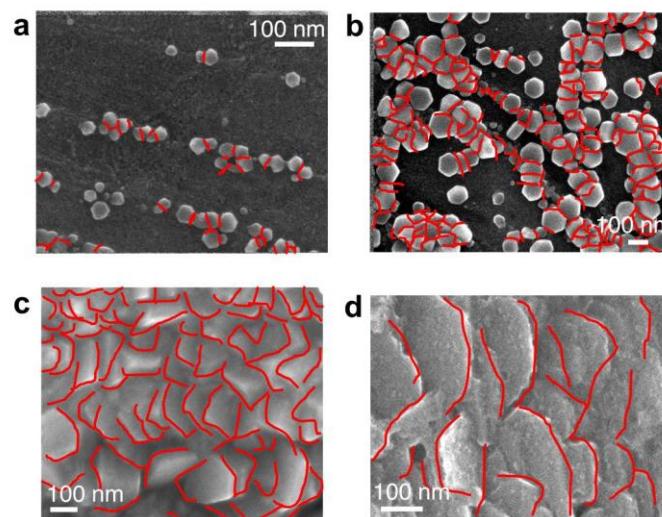

Figure S3. Evaluation of number of hot spots between NHCs for reaction times of (a) 1, (b) 3, (c) 30, and (d) 100 min. Red lines indicate each crevice.

Table 2. Number of hot spots between NHCs on the SERS substrates for reaction times of 1, 3, 30 and 100 min.

Reaction time (min)	Number of hotspots [a] / 1.93 µm^2 [b]
1	154 ± 22
3	240 ± 14
30	168 ± 6
100	104 ± 19

[a] mean ± SD (n=3). [b] Focal area of objective used (NA 0.4).

(5) Solution-by-solution variations and Substrate-by-substrate variations in SERS intensities

The present reaction of thiosulfate-silver complexes $[Ag(S_2O_3)_n]^{-(2n-1)}$ and phosphor bronze substrate shows well reproducibility in SERS intensities produced by NHCs. However, we were not able to quantitatively achieve the temporal profiles after leaving thiosulfate-silver solution for several months or changing lots of phosphor bronze. In particular, the number of NHC on the substrate is less than the original experiments so that SERS intensities were lower than previous experiments.

To clarify the problem, we carefully observed the thiosulfate-silver solution for a long time and found that Ag bulk particles have been precipitated within several months. Thus, the less number of NHC may be due to the decreasing in the concentration of Ag$^+$ ion by the

precipitation. We also found that the precipitation itself shows solution-by-solution variations, indicating the stability of thiosulfate-silver solution varies. Thus, we consider that the solution-by-solution variations in SERS intensities are induced by intrinsic instability of thiosulfate-silver solution.

We also found substance-by-substance variations in SERS intensities. In particular, substances made from different lot of phosphor bronze exhibited large variations. Thus, we consider that the contents variation may be the origin of the variations. The contents of phosphor bronze follow Japanese Industrial Standards (JIS) H3110, C5191P (Sn 5.5~7.0%, P 0.03~0.35%, Cu residual). JIS is a protocol of a standardization for industrial activities in Japan and we decided to use the material for future industrial usage. However, as indicated in JIS no. C5191P, the ranges of percentage of each content are too wide for Galvanic displacement, which is sensitive to surface potential. Indeed, the generation of NHCs cannot be observed on pure Cu substrates, even ~95% of phosphor bronze is composed of Cu. Thus, we consider that the substance-by-substance variations is induced by the variation of the contents of phosphor bronze lots.

(6) SERS intensity of R6G and CR on NHCs

Figure S4a shows that the SERS intensity of R6G is several times higher than that of CR on the NHCs. Before discussing this difference in SERS intensity, we briefly explain the two SERS models, namely, the electromagnetic (EM) and charge-transfer (CT) models.[11,12] The EM model is characterized by a twofold EM enhancement induced by the coupling of plasmon resonance with both incident and Raman light.[13] CT enhancement is characterized by a change from nonresonant Raman scatteringto resonant scattering through the formation of CT complexes between the adsorbed molecules and the metal surface.[14] In other words, CT resonance is the origin of the enhancement in the CT model. In the case of dye molecules like R6G and CR, the EM model is dominant, because optical resonance Raman effects induced by electronic transitions in π-electron systems make the CT resonance effect in SERS negligible.[13,15] Indeed, the CT model is usually observed in specific target molecules, e.g., pyridine, that do not resonate in the visible light region.[16] Furthermore, we have demonstrated that the SERS of R6G can be accurately reproduced using the EM model.[13] Thus, we expect that the SERS from R6G and CR can be rationalized using the EM model because of their strong resonance Raman effects.

Figures S4b and S4c show that the optical absorption band of CR is closer to the Raman excitation wavelength of 633 nm than that of R6G. Thus, the SERS intensity of CR is expected to be larger than that of R6G, even though the peak absorption cross section of R6G (2.0×10^{-16} cm^2) is larger than that of CR (7.5×10^{-17} cm^2). Indeed, the absorbance of CR at 570 nm is larger than that of R6G. Thus, the SERS intensity of CR is expected to be larger than that of R6G. However, Fig. S4a shows that SERS intensity of CR is weaker. This unexpected result is attributed to the difference between the affinities of the dye molecules for the NHCs, because EM enhancement is quite sensitive to the distance between the molecules and the hot spots, usually requiring distance to be within a few nanometers.[13,15,17] In other words, we believe that the R6G molecules can approach the hot spots more closely than the CR molecules. This is reasonable, because as suggested in the communication in Eq. 3, the surfaces of the NHCs are completely covered with ions containing sulfur, possibly thiosulfates. Therefore, the NHCs' surfaces are negatively charged, so R6G (a cationic dye) can approach closer to the hot spots on the NHCs and generate a stronger SERS signal than CR (an anionic dye). Overall, we expect that the NHCs are negatively charged because of the ions containing sulfur on their surfaces. This means that NHCs selectively attract cationic molecules, e.g., R6G, which therefore generate a stronger SERS signal than anionic molecules, e.g., CR.
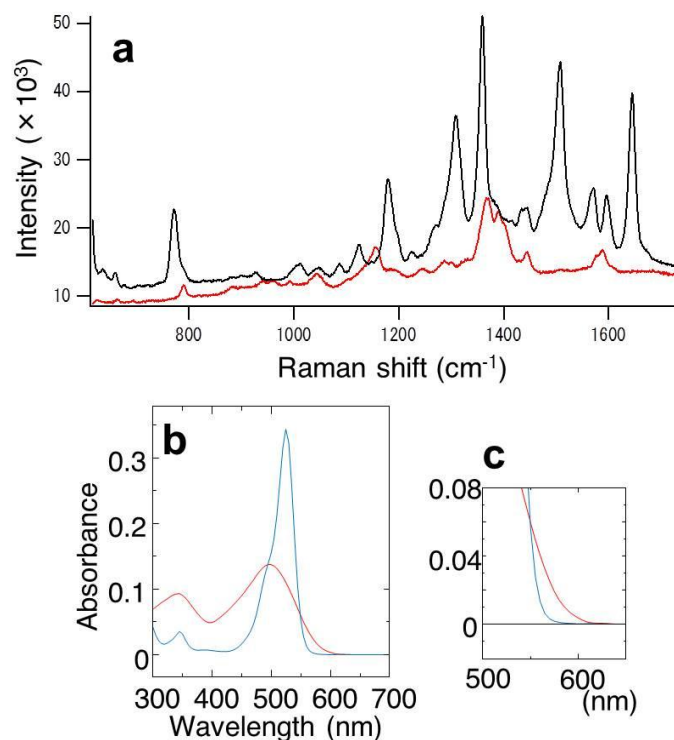
Figure S4. (a) Comparison of SERS spectra from R6G (3×10^{-6} M, black) and CR (3×10^{-6} M, red) added to NHCs. Absorption spectra of R6G (blue) compared with those of CR (red) at (b) low and (c) high magnification.

References for Supporting Information

1   L. Rintoul, K. Crawford, H. F. Shurvell, and P. M. Fredericks, *Vib. Spectrosc.* 1997, **15**, 171.
2   R. Narayanan and M. A. El-Sayed, *J. Phys. Chem. B* 2005, **109**, 18460.
3   E. C. Le Ru, E. Blackie, M. Meyer and P. G. Etchegoin, *J. Phys. Chem. C* 2007, **111**, 13794.
4   A. Gutes, C. Carraro and R. Maboudian, *ACS Appl. Mater. Interf.* 2009, **1**, 2551.
5   K. C. Grabar, R. G. Freeman, M. B. Hommer and M. J. Natan, *Anal. Chem.* 1995, **67**, 735.
6   L. Rivas, S. Sanchez-Cortes, J. V. Garcia-Ramos and G. Morcillo, *Langmuir* 2000, **16**, 9722.
7   K. Yoshida, T. Itoh, H. Tamaru, V. Biju, M. Ishikawa and Y. Ozaki, *Phys. Rev. B Condens. Matter Mater. Phys.* 2010, **81**, 115406.
8   M. Moskovits, Rev. Mod. Phys. 1985, **57**, 783.
9   P. Johansson, H. Xu and M. Käll, *Phys. Rev. B Condens. Matter Mater. Phys.* 2005, **72**, 035427.
10   T. Itoh, V. Biju, M. Ishikawa, Y. Kikkawa, K. Hashimoto, A. Ikehata and Y. Ozaki, *J. Chem. Phys.* 2006, **124**, 134708.

11   D. S. Wang and M. Kerker, *Phys. Rev. B Condens. Matter Mater. Phys.* 1981, **24**, 1777.
12   M. G. Albrecht and J. A. Creighton, *J. Am. Chem. Soc.* 1977, **99**, 5215.
13   K. Yoshida, T. Itoh, H. Tamaru, V. Biju, M. Ishikawa and Y. Ozaki, *Phys. Rev. B Condens. Matter Mater. Phys.* 2010, **81**, 115406.
14   D. Y.Wu, J. F. Li, B. Ren and Z. Q. Tian, *Chem. Soc. Rev.* 2008, **37**, 1025.

15   P. Johansson, H. X. Xu and M. Käll, *Phys. Rev. B Condens. Matter Mater. Phys.* 2005, **72**, 035427.

16   A. Campion and P. Kambhampati, *Chem. Soc. Rev.* 1998, **27**, 241.

17   P. G. Etchegoin and E. C. Le Ru, *Anal. Chem.* 2010, **82**, 2888–2892.